Signaling kinetics of DNA and aptamer biosensors revealing graphene oxide surface heterogeneity

Po-Jung Jimmy Huang and Juewen Liu*

Department of Chemistry, Waterloo Institute for Nanotechnology, University of Waterloo, Waterloo, Ontario, N2L 3G1, Canada

Email: liujw@uwaterloo.ca

Abstract.

Adsorption of fluorescently labeled DNA and aptamer probes to graphene oxide (GO) has been one of the most popular methods for developing biosensors. In the presence of target analytes, the quenched fluorescence would recover. In this work, we followed the kinetics of the reactions and found that the fluorescence would eventually drop after an initial increase, and this was attributed to the re-adsorption of the desorbed probe DNA molecules. Both a DNA probe and an aptamer for adenosine were used. This re-adsorption was attributed to the surface heterogeneity of GO, and the DNA probes desorbed from relatively weaker binding sites were re-adsorbed on the stronger binding sites. This re-adsorption can be avoided by extensive washing the samples, and also by blocking the GO surface or by heating. This fundamental understanding is important for achieving a stable signal of such biosensors.

Keywords: kinetics, DNA, aptamer, biosensors, graphene

1. Introduction

Adsorption and desorption of biopolymers from inorganic surfaces is a fundamental process in nanotechnology [1-5]. Applications related to biosensor development, biomaterials design, drug delivery, and catalysis can all be linked to and are sometimes even governed by interfacial properties [6]. As a result, adsorption of proteins and DNA on many surfaces has been extensively studied including gold [7], polymers [8], silica [9], and metal oxide surfaces [3]. These surfaces are relatively homogeneous at the length scale of a few nanometers (e.g. the size of typical DNA oligonucleotides or proteins).

Graphene oxide (GO) is highly popular for developing biosensors [10-14]. The surface of GO is described to contain both crystalline carbon domains where the structure of pristine graphene is preserved, and highly oxidized regions containing surface hydroxyl and carboxylic acid groups [15-17]. With these hydrophilic groups, GO can be easily dispersed in water. Such nano-domain structures are not available in most other surfaces.

In a relatively high ionic strength buffer, GO can strongly adsorb single-stranded (ss) DNA molecules and effectively quench adsorbed fluorophores [1, 4]. DNA is negatively charged at neutral pH and so is GO. Thus, a high salt buffer is required to screen the repulsive forces. For a well-folded or double-stranded (ds) DNA, whose nucleobases are shielded, DNA adsorption by GO is significantly reduced [18-22]. Based on these interactions, a general optical sensing method has been developed as shown in Figure 1. A fluorophore-labeled probe DNA or aptamer is first adsorbed on GO to result in quenched fluorescence. Addition of its cDNA or the aptamer target induces probe desorption and fluorescence recovery [1, 23]. A variation of this scheme is to pre-mix DNA probes with target molecules followed by adding GO [24, 25]. In the presence of the target, the probe adsorption by GO is slower and a fluorescence difference can also be achieved. These methods have been applied for the detection of nucleic acids [1, 24, 26-29], proteins [30, 31], virus [32], metal ions [25], and small molecules [33-35] showing good generality.

Most of the biosensor work reported only end-point fluorescence intensities while little kinetic information was given [36]. Studying reaction kinetics can provide important mechanistic insights into surface reactions and may allow further optimization of sensor performance. In this work, we observed very intriguing kinetic profiles for DNA/GO based biosensors. The sensor fluorescence initially increased upon target addition, but it was followed by a fluorescence decay. This unstable kinetics makes accurate detection more difficult. After extensive studies, we attribute this intriguing kinetics to GO surface heterogeneity (i.e. the presence of nanoscale domains with different DNA adsorption affinities) [16]. We proposed that DNA binding to the carbon-rich regions was much stronger, and

DNA can migrate from low affinity domains to high affinity ones in the presence of target molecules. Based on this understanding, we were able to minimize this unstable kinetics. This study provides a better picture about GO surface interacting with biomolecules and will help rational design of GO-based biosensors.

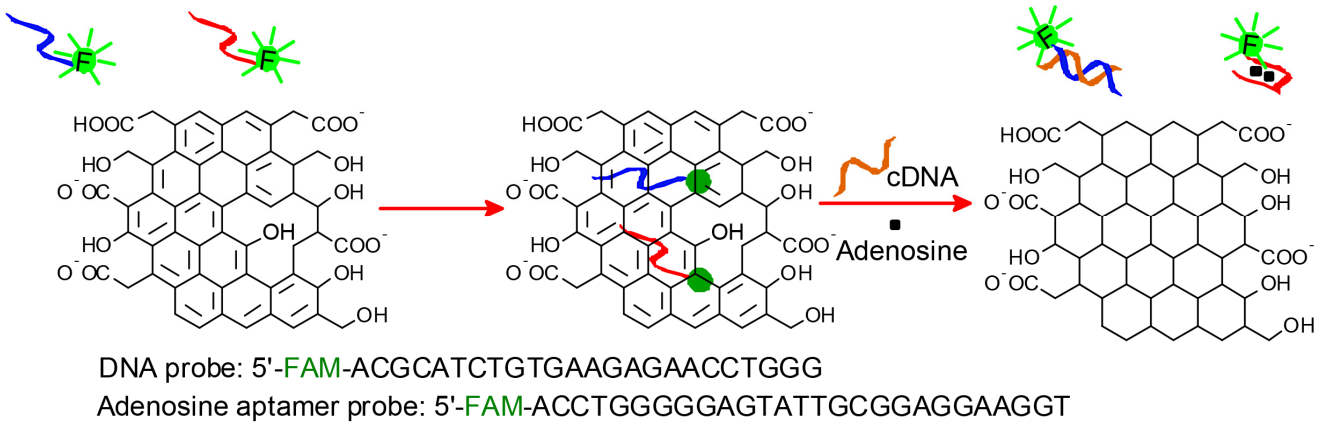


Figure 1. Schematics of fluorescent biosensors based on GO and DNA or aptamer probes. Upon probe adsorption, the fluorescence is quenched. By adding the cDNA or adenosine, the probe DNAs are desorbed to restore the fluorescence signal. The DNA probe sequences used in this study are also shown.

2. Experimental Section.

2.1. Chemicals. All DNA samples were purchased from Integrated DNA Technologies (Coralville, IA). The sequences of the DNA are: carboxyfluorescein (FAM)-labeled 24-mer DNA: FAM-ACGCATCTGTGAAGAGAACCTGGG-3′, its cDNA: CCCAGGTTCTCTTCACAGATGCGT-3′; FAM-labeled adenosine aptamer: FAM-ACCTGGGGGAGTATTGCGGAGGAAGGT-3′; and FAM-labeled Hg^{2+} binding DNA as a control sequence: FAM-TTCTTTCTTCCCCTTGTTTGTT. Sodium chloride, magnesium chloride, 4-(2-hydroxyethyl)piperazine-1-ethanesulfonate (HEPES), adenosine, uridine, guanosine, and cytidine were purchased from Mandel Scientific (Guelph, Ontario, Canada). Carboxyl GO was purchased from ACS Material Inc. Millipore water was used to prepare all the solutions and buffers.

2.2. Physical adsorption of DNA on GO. In a typical experiment, 500 nM (or other DNA concentrations tested) of the FAM-labeled probe DNA was incubated with 100 μg/mL GO in buffer (25 mM HEPES, pH 7.6 with designated salt concentrations) for 1 h at room temperature. Any non-adsorbed DNA was removed by centrifugation and purified GO/DNA complex was dispersed in the buffer.

2.3. Detection of DNA and adenosine. The kinetics of fluorescence increase was measured using a fluorescence microplate reader (Infinite F200 Pro, Tecan) under the FAM channel. In each well, 50 μL of the sensor (GO concentration 20 μg/mL) in buffer was added. After monitoring the background fluorescence for around 10 min, a small volume (usually <5 μL) of target DNA or adenosine was added and the fluorescence was monitored every 10 sec for 30 min to 3 h. cDNA were prepared with 5 mM HEPES buffer and adenosine were prepared with Milli-Q water. For testing the specificity of the adenosine aptamer sensor, 500 μM adenosine, guanosine, cytidine or uridine was added to 50 μL of the sensor. Due to the low solubility of guanosine and adenosine, both solutions were pre-heated before the addition. Guanosine was prepared at a concentration of 5 mM and the other ones were at 50 mM.

3. Results and Discussion

3.1. Sensor signaling kinetics. To systematically study the signaling kinetics, two different sensors were tested for the detection of a biopolymer (DNA) and a small molecule (adenosine), respectively. To prepare the sensors, each FAM-labeled probe DNA was mixed with GO in a high salt buffer for adsorption. For DNA detection, a 24-mer probe DNA with a 5′-FAM label was used. In the absence of its complementary DNA (cDNA), a very low and stable background was observed (Figure 2A, red curve), suggesting that the adsorption was strong. Addition of the cDNA resulted in a concentration-dependent fluorescence increase. At each target concentration, the fluorescence initially increased followed by a slow decay. Next, a FAM-labeled adenosine aptamer was adsorbed on the GO surface (see Figure 1A for the DNA sequence), where adenosine resulted in a similar initial signal increase followed by a slow decay phase (Figure 2B). The signal decay phase cannot be attributed to photobleaching since under the same experimental conditions, no decay was observed if the DNA sensor was prepared in a different way (*vide infra*). For practical analytical applications, the decaying signal is undesirable. Normally, for such binding-based assays, a stable signal can be expected after an equilibrium is reached. The similar kinetic behavior for both the DNA and the aptamer systems suggests a common mechanism that is independent of the target molecule species. The decay of signal

is intriguing and suggests the presence of a more complex kinetic behavior that warrants a more careful study.

In both sensor systems, only the probe DNAs were fluorescently labeled. Since GO can completely quench the adsorbed fluorophore, the increased fluorescence suggested probe desorption and the subsequent decay phase can only be attributed to probe re-adsorption.

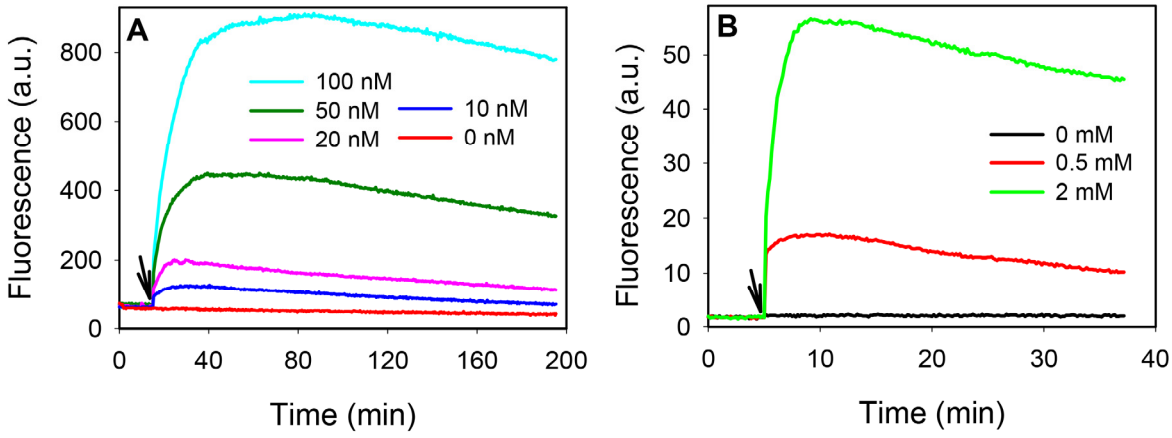


Figure 2. Signaling kinetics of the DNA probes for the detection of (A) cDNA, and (B) adenosine. The target analytes were added at the time points indicated by the arrows. The DNA binding kinetics was slower and therefore monitored for a longer time. Ionic strength: 150 mM NaCl, 1 mM Mg^{2+}; GO concentration: 20 μg/mL.

3.2. Adenosine detection as a function of salt concentration. We then chose to use the adenosine probe to carry out systematic studies since it has relative fast reaction kinetics. In addition, there are several other ribonucleosides that can be used to test specificity and further understand the desorption mechanism. DNA adsorption/desorption on GO can be conveniently controlled by tuning the ionic strength [4]. The sensor was first dispersed in a low salt buffer (150 mM NaCl and 25 mM HEPES, pH 7.6) and 0.5 mM of various nucleosides were added. Interestingly, we observed a similar signal increase for adenosine (**A**) and guanosine (**G**), while cytidine (**C**) or uridine (**U**) showed little response (Figure 3A). This aptamer is known to have no affinity for **G** [37], and thus this signal increase can only be attributed to the non-specific displacement of the aptamer by **G**. Therefore, when the interaction between DNA and GO was relatively weak (e.g. in a low salt buffer), and non-specific displacement of the probe DNA due to target/GO interactions can dominate the system. Such target/surface interactions have also been observed in other systems such as metal oxides [23] and gold

[38-40] as well. After the initial fluorescence signal spike, the decay of fluorescence was observed for both **A** and **G**, suggesting re-adsorption of the desorbed aptamer probes.

It is known that DNA adsorption to GO is much stronger in the presence of divalent metal ions such as Mg^{2+} [4]. Next, 1 mM $MgCl_2$ was added to the buffer (in addition to the 150 mM NaCl). Addition of the nucleosides resulted in a slightly different pattern as shown in Figure 3B. Compared to the previous Mg^{2+}-free system, the overall fluorescence signal was lower for both **A** and **G**. The initial spike reached a fluorescence reading of ~30 for **G** in the Mg^{2+} free buffer but only ~10 when Mg^{2+} was present. This observation supported that the aptamer was more tightly adsorbed by GO in the presence of Mg^{2+} and thus non-specific displacement by **G** was reduced. Although the signal in the presence of **A** was also reduced, the difference between **A** and **G** became much larger. This could be attributed to the better binding of the aptamer in the presence of a higher salt concentration [39]. The signal decay phase was also observed for both **A** and **G** under this condition.

Since adding 1 mM Mg^{2+} appeared to improve selectivity towards the aptamer target, the salt was further raised to contain 4 mM Mg^{2+}. As can be observed from Figure 3C, however, the sensor performance actually decreased. For **G**, the signal reached a steady value very quickly and the absolute fluorescence increase was even lower (e.g. final fluorescence = ~5), which is consistent with the further reduced non-specific displacement. The signal difference between **A** and **G** became very small. This indicated that the aptamer/GO binding was stronger than aptamer/adenosine binding and most of the desorbed aptamers re-associated with the GO surface under such a high Mg^{2+} condition.

The adenosine aptamer tested above can selectively bind to **A** but not **G**. The increase of fluorescence in the presence of **G** indicated that **G** can effectively compete with DNA for surface binding sites. To quantitatively understand the non-specific binding, we added the nucleosides to another FAM-labeled DNA (i.e. the Hg^{2+} binding DNA). This DNA is not an aptamer for either **A** or **G** and therefore any fluorescence increase can only be attributed to non-specific displacement. As shown in Figure 3D, **G** showed a slightly higher fluorescence signal than **A**, suggesting that it had a higher binding affinity to the GO surface. The higher affinity for **G** has also been observed previously using isothermal titration calorimetry (ITC) [41]. The fact that no fluorescence increase was observed in the presence of **U** or **C** confirmed that the binding to pyrimidines were much weaker compared to that for purines [41-43]. Interestingly, the decay pattern was still observed for this control DNA.

This salt-dependent kinetic study revealed some important features of physically adsorbed aptamer probes. First, non-specific displacement of the adsorbed aptamer probe can occur, which can lead to false positive results. For example, both **G** and **A** at a moderate concentration of 0.5 mM can

effectively displace adsorbed DNA. This is a practical concern for cellular or blood related applications, since there are many other small molecule metabolites, nucleic acids and proteins that can compete for the surface binding sites on GO. Therefore, the observed signal may not be exclusively due to the intended target. Second, careful optimization work needs to be carried out under different detection conditions. For example, we observed a relatively large difference between **A** and **G** with 1 mM Mg^{2+} but not with 0 or 4 mM Mg^{2+}. If the adsorption of the aptamer probe was too weak, non-specific displacement dominated the signal. On the other hand, if the adsorption was too strong, little signal was generated. This experiment, however, did not provide enough insights to explain why decayed signal was observed. To understand this, we performed the following experiments.

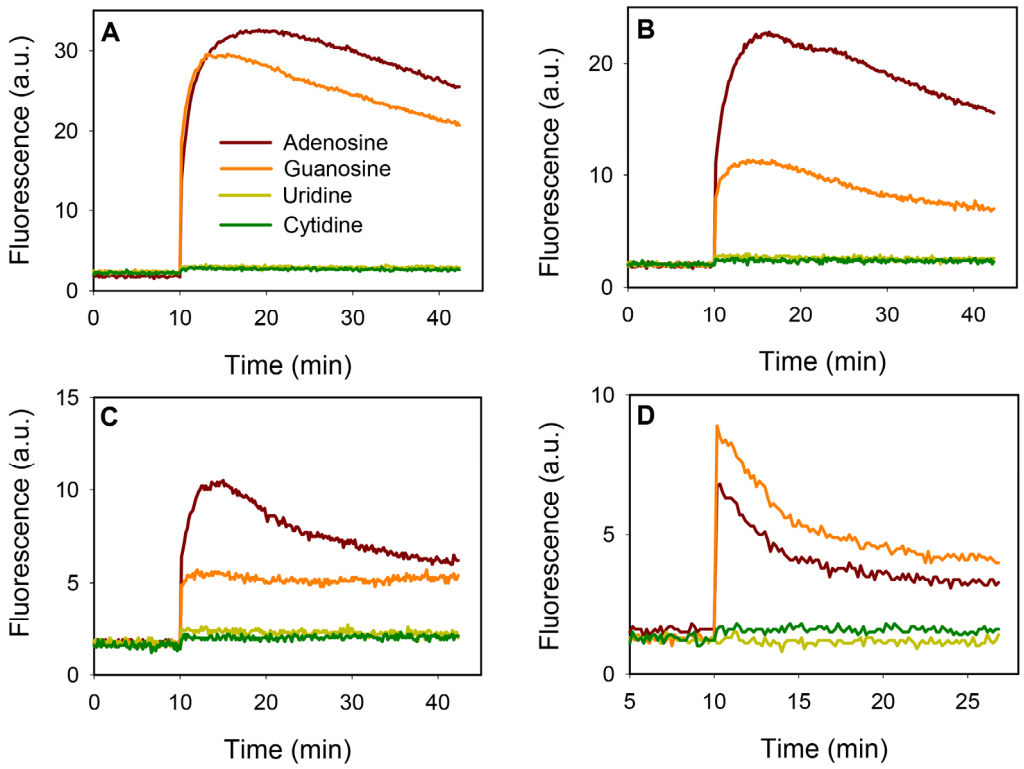


Figure 3. Kinetics of fluorescence signal change of (A-C) the FAM-labeled adenosine aptamer probe, and (D) the Hg^{2+} binding DNA adsorbed on GO in the presence of 0.5 mM **A**, **G**, **U**, or **C**. Buffer conditions: (A) 150 mM NaCl; (B) 150 mM NaCl, 1 mM $MgCl_2$; (C) 150 mM NaCl, 4 mM $MgCl_2$; (D) 150 mM NaCl, 4 mM $MgCl_2$. All the figure panels here share the same legends in (A).

3.3. Effect of sensor/target concentration. It can be observed from the above experiments that **A** and **G** can strongly adsorb on GO. Therefore, one explanation for the decay part of the kinetic traces is that the added GO decreased the concentration of **A** and **G** in solution. For example, the initial

concentration of **A** in solution was 0.5 mM, which can desorb a certain amount of the DNA probe via formation of the aptamer/adenosine binding complex. The desorbed probe had to bind to **A** in solution to avoid re-adsorption by GO. With **A** in solution being adsorbed by GO, its concentration was reduced, leading to some aptamers in solution losing the bound **A** due to the shift of the chemical equilibrium and re-adsorption of these aptamers. This may explain the decay part of the kinetic traces for **A**.

To test this hypothesis, first, if 0.5 mM **A** or **G** was added to a more diluted sensor (5 instead of 20 μg/mL GO), we indeed observed a much more stable signal for both samples (Figure 4A). Second, if 2 mM **A** or **G** was added to 5 μg/mL GO, no more decay was observed (Figure 4B). This suggested that our hypothesis was correct in terms of target adsorption by GO, leading to a reduced **A** concentration in solution to shift the reaction equilibrium between the aptamer, adenosine, and GO. With a low concentration of GO and high concentration of target, even after saturating all the surface binding sites with **A**, there were still a sufficient concentration of **A** in solution to keep the desorbed aptamer in the binding state.

This mechanism, however, cannot explain why **G** also induced a decayed fluorescence, since there was no specific binding between **G** and the aptamer. After the initial desorption via non-specific displacement, as more **G** molecules were adsorbed on the surface, more DNA desorption should have occurred, leading to increased instead of decreased fluorescence.

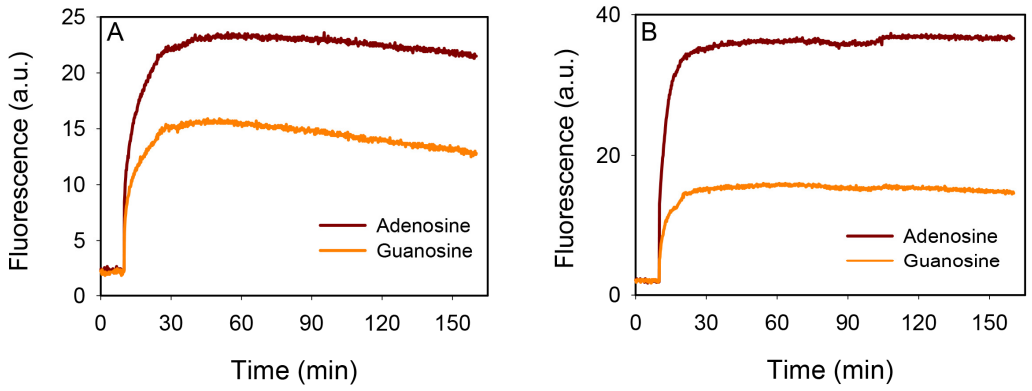


Figure 4. Kinetics of fluorescence signal change with the FAM-labeled adenosine aptamer probe. (A) 5 μg/mL GO with 0.5 mM **A** or **G**; (B) 5 μg/mL GO with 2 mM **A** or **G**. Both samples contained 1 mM Mg^{2+} and 150 mM NaCl in the buffer.

3.4. Effect of washing. In the above sensor preparation, no washing step was performed. After mixing the DNA probes with GO, almost all the probes were adsorbed, resulting in very low background

fluorescence. We found that we can eliminate the decaying part of the kinetic traces after washing the sensors with water. In water, the ionic strength was very low and weakly adsorbed DNAs were likely to desorb. As discussed previously, the GO surface contains both highly oxidized regions and highly crystalline carbon rich regions. We expected that the weakly adsorbed DNAs were on the oxidized regions since these regions were also negatively charged [44]. A high ionic strength was required to screen the repulsive force with DNA. On the other hand, DNA strands adsorbed on the carbon-rich regions should be less affected by ionic strength since the interaction should be of hydrophobic nature. As shown in Figure 5A, with a high concentration of 20 μg/mL GO and 4 mM $MgCl_2$ (the same condition as in Figure 3C), after washing treatment, we did not observed any decayed signal in the presence of both **A** and **G**. After washing in water, the same observation was also made for the detection of cDNA as shown in Figure 5B.

3.5. Surface heterogeneity. We can explain all the experimental results by considering the surface heterogeneity of GO. GO is composed of nanoscale domains. DNA binding to the crystalline carbon regions is likely to be stronger due to a lack of electrostatic repulsion [17]. In the more oxidized regions, there are a lot of negative charges and DNA binding is weaker. DNA probes were initially adsorbed on both the high affinity and low affinity regions. Even though there was a difference in the binding affinity, the adsorption was still very strong even for the low affinity sites. This can be deduced from thermal desorption experiments reported previously. For example, with a moderate salt buffer (e.g. 200 mM NaCl), almost no thermal dissociation of DNA occurred [4, 27, 45]. At very low salt conditions, thermal desorption can be observed, but there were no obvious melting transitions and DNA desorption occurred over a wide temperature range, indicating the presence of a wide variety of sites with different binding affinities [4, 46]. The tight adsorption makes on-surface diffusion difficult.

Addition of **G** caused desorption of some of the less tightly adsorbed DNA probes due to non-specific displacement. The desorbed DNA can still be re-adsorbed. This time, however, the DNA had to choose to be adsorbed on higher affinity sites, since at lower affinity sites they would be desorbed again. The final result was that more DNAs were on the higher affinity sites than that in the initial distribution. After washing, the weakly adsorbed DNAs were removed and only the strongly adsorbed ones remained on the surface. Addition of **G** or **A** induced desorption of some of these DNAs but they cannot migrate to other sites; the situation became a simple desorption reaction and no re-adsorption occurred.

The fact that signal decay was still observed for the 24-mer DNA target indicated that the binding between DNA and GO can be so strong that even 24-mer DNA cannot compete with the high

affinity regions. If the sensor sample was washed, no decay was observed as shown in Figure 5B, further confirming the generality of our observation.

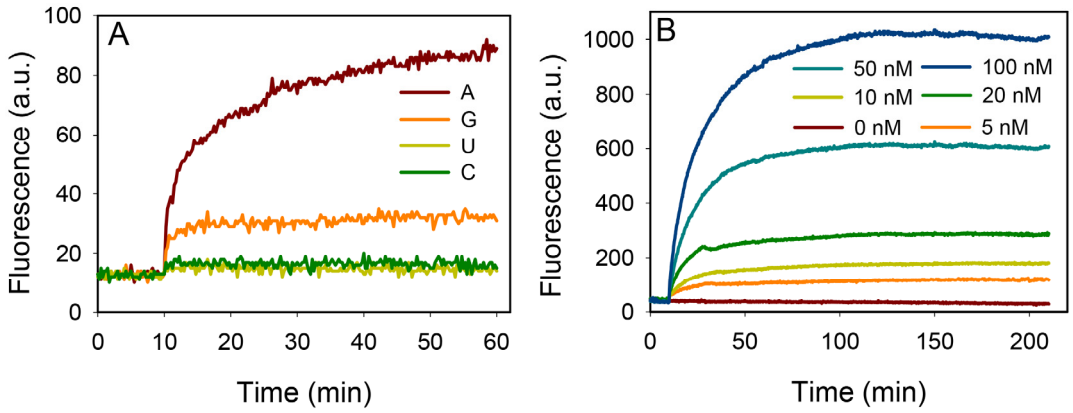


Figure 5. Signaling kinetics of the DNA/GO sample washed in water for the detection of (A) adenosine, and (B) cDNA. Ionic strength: 150 mM NaCl 1 mM Mg^{2+}; GO concentration: 20 μg/mL.

3.6. Target induced migration of probe DNA. At this point, we can summarize the reaction mechanism as shown in Figure 6. There are two types of regions on GO with different DNA binding affinity. Practically, this is unlikely to be a clear cut, and regions with intermediate affinities should also exist. Mixing DNA and GO results in DNA adsorption. Although the adsorption affinity differs at the different regions, the binding even at low affinity sites is still very strong. Therefore, thermal energy at room temperature is insufficient to spontaneously move all the DNAs to the higher affinity sites. In other words, this system is kinetically trapped. Addition of molecules that can either interact with DNA (e.g. cDNA and **A**) or the surface (e.g. **G**) resulted in a perturbation in the system to desorb some of the probe DNAs. DNAs on the lower affinity regions should be the first ones to desorb. Since there were still free surface sites with high affinity to accept incoming DNAs, re-adsorption is observed (the fluorescence decay part).

The GO surface is unique in terms of its nano-sized domains. The domain sizes are large enough to accommodate several DNA molecules. Other commonly used surfaces such as silica and gold do not possess such features; their surface properties are more homogeneously distributed. It needs to be noted that we attributed our observations to surface heterogeneity of GO only based on the kinetics of the sensors. We could not fully rule out other possibilities, but we believe this is a reasonable hypothesis.

In terms of practical applications, the surface heterogeneity needs to be noted for biosensor development. The perturbation effect of GO in terms of non-specific target adsorption can hardly be avoided. We have demonstrated that heating can also drive DNA to higher affinity regions [17]. Another way is to block the surface [1, 47]. Finally, as demonstrated in this work, it can be improved by washing. Among the three methods including washing, blocking and heating that can achieve stable signals, blocking might be the most robust method, since it can increase the efficiency of using the target DNA.

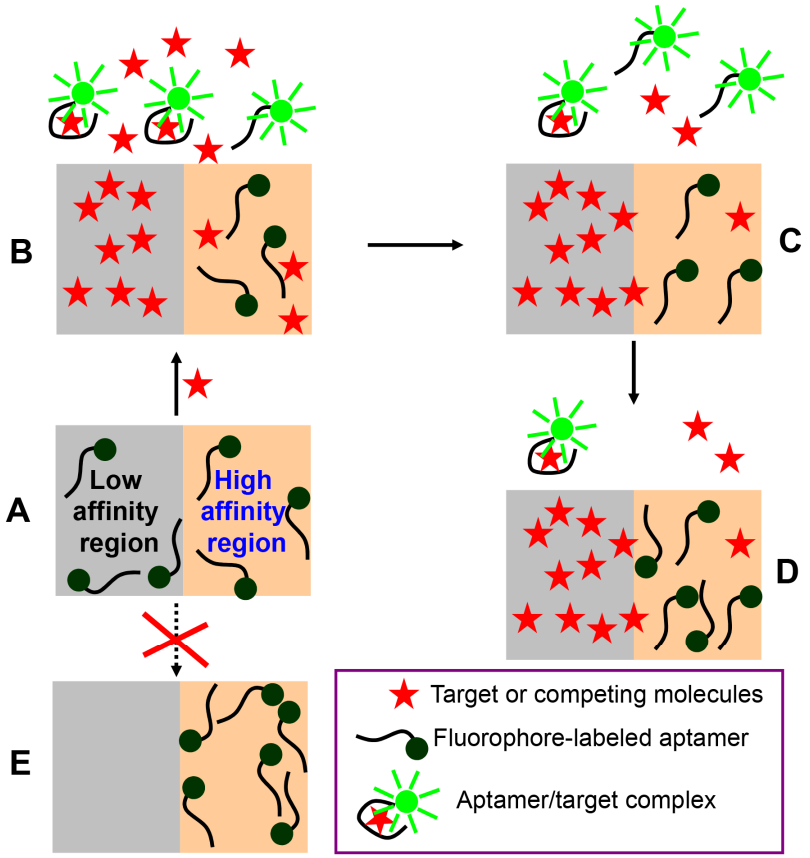


Figure 6. Schematics of aptamer adsorption/desorption on GO induced by target molecules. (A) Probe DNAs are randomly adsorbed on the GO surface with fluorescence being quenched. Both the low affinity and high affinity regions contain adsorbed DNA. (B) Addition of the target molecule (denoted by a red star) resulted in desorption and fluorescence enhancement. (C) The target can also be adsorbed on the GO surface, reducing the concentration in solution, leading to releasing of the target by aptamers in solution and re-adsorption of the aptamer to the higher affinity sites (D). (E) The DNAs are tightly adsorbed and cannot spontaneously diffuse to the high affinity sites.

4. Conclusions

From this work the following conclusions can be reached. The initial DNA adsorption on GO is quite random and can occur on both high affinity and low affinity regions. The reason is that even for low affinity regions, the binding is still quite strong. Under chemical perturbation, DNA can desorb into solution and be re-adsorbed at higher affinity sites, resulting in an unstable kinetic behavior. After washing in water, weakly bound DNAs are removed and the decaying part can be eliminated. This work shows the importance of understanding the fundamental interactions between biomolecules and inorganic surfaces, and GO provides an ideal platform for such studies. Such understandings are useful for improving biosensors.

Acknowledgements

Funding for this work was from the Natural Sciences and Engineering Research Council of Canada (NSERC).

References

[1] C. H. Lu; H. H. Yang; C. L. Zhu; X. Chen; G. N. Chen, A graphene platform for sensing biomolecules. Angew Chem Int Ed. 2009;48:4785-7.

[2] A. Lopez; J. Liu, Covalent and noncovalent functionalization of graphene oxide with DNA for smart sensing. Adv Intell Sys. 2020;2:2000123.

[3] B. Liu; J. Liu, Sensors and biosensors based on metal oxide nanomaterials. TrAC, Trends Anal Chem. 2019;121:115690.

[4] M. Wu; R. Kempaiah; P.-J. J. Huang; V. Maheshwari; J. Liu, Adsorption and desorption of DNA on graphene oxide studied by fluorescently labeled oligonucleotides. Langmuir. 2011;27:2731–8.

[5] X. X. Shi; H. Xu; Y. N. Wu; Y. M. Zhao; H. M. Meng; Z. H. Li; L. B. Qu, Two-dimension (2D) Cu-MOFs/aptamer nanoprobe for in situ atp imaging in living cells. J Anal Test. 2021;5:165-73.

[6] J. B. Schlenoff, Zwitteration: Coating surfaces with zwitterionic functionality to reduce nonspecific adsorption. Langmuir. 2014;30:9625-36.

[7] B. Liu; J. Liu, Interface driven hybrid materials based on DNA-functionalized gold nanoparticles. Matter. 2019;1:825-47.

[8] M. Zandieh; B. M. Hagar; J. Liu, Interfacing DNA and polydopamine nanoparticles and its applications. Part Part Syst Char. 2020;37: 2000208.

[9] P. E. Vandeventer; J. Mejia; A. Nadim; M. S. Johal; A. Niemz, DNA adsorption to and elution from silica surfaces: Influence of amino acid buffers. J Phys Chem B. 2013;117:10742-9.

[10] L. H. Tang; Y. Wang; J. H. Li, The graphene/nucleic acid nanobiointerface. Chem. Soc. Rev. 2015;44:6954-80.

[11] B. Liu; S. Salgado; V. Maheshwari; J. Liu, DNA adsorbed on graphene and graphene oxide: Fundamental interactions, desorption and applications. Curr Opin Colloid Interface Sci. 2016;26:41-9.

[12] J. Peña-Bahamonde; H. N. Nguyen; S. K. Fanourakis; D. F. Rodrigues, Recent advances in graphene-based biosensor technology with applications in life sciences. J Nanobiotechnol. 2018;16:75.

[13] J. S. Tabunag; Y. J. Guo; H. Z. Yu, Interactions between hemin-binding DNA aptamers and hemin-graphene nanosheets: Reduced affinity but unperturbed catalytic activity. J Anal Test. 2019;3:107-16.
[14] S. Su; Q. Sun; X. D. Gu; Y. Q. Xu; J. L. Shen; D. Zhu; J. Chao; C. H. Fan; L. H. Wang, Two-dimensional nanomaterials for biosensing applications. TrAC Trends Anal Chem. 2019;119.
[15] A. Lerf; H. He; M. Forster; J. Klinowski, Structure of graphite oxide revisited. The Journal of Physical Chemistry B. 1998;102:4477-82.
[16] C. Gomez-Navarro; J. C. Meyer; R. S. Sundaram; A. Chuvilin; S. Kurasch; M. Burghard; K. Kern; U. Kaiser, Atomic structure of reduced graphene oxide. Nano Lett. 2010;10:1144-8.
[17] B. Liu; Y. Zhao; Y. Jia; J. Liu, Heating drives DNA to hydrophobic regions while freezing to hydrophilic regions of graphene oxide for highly robust biosensors. J. Am. Chem. Soc. 2020;142:14702–9.
[18] M. P. Kushalkar; B. Liu; J. Liu, Promoting DNA adsorption by acids and polyvalent cations: Beyond charge screening. Langmuir. 2020;36:11183–95.
[19] D. F. Becheru; G. M. Vlăsceanu; A. Banciu; E. Vasile; M. Ioniţă; J. S. Burns, Optical graphene-based biosensor for nucleic acid detection; influence of graphene functionalization and ionic strength. Int J Mol Sci. 2018;19:3230.
[20] A. Lopez; Y. Zhao; Z. C. Huang; Y. F. Guo; S. K. Guan; Y. Jia; J. W. Liu, Poly-cytosine deoxyribonucleic acid strongly anchoring on graphene oxide due to flexible backbone phosphate interactions. Adv Mater Interfaces. 2021;8: 2001798.
[21] Z. C. Huang; Y. Zhao; B. W. Liu; S. K. Guan; J. W. Liu, Stronger adsorption of phosphorothioate DNA oligonucleotides on graphene oxide by van der waals forces. Langmuir. 2020;36:13708-15.
[22] J. Lee; Y. Yim; S. Kim; M.-H. Choi; B.-S. Choi; Y. Lee; D.-H. Min, In-depth investigation of the interaction between DNA and nano-sized graphene oxide. Carbon. 2016;97:92-8.
[23] A. Lopez; J. Liu, Nanomaterial and aptamer-based sensing: Target binding versus target adsorption illustrated by the detection of adenosine and ATP on metal oxides and graphene oxide. Anal Chem. 2021;93:3018-25.
[24] S. J. He; B. Song; D. Li; C. F. Zhu; W. P. Qi; Y. Q. Wen; L. H. Wang; S. P. Song; H. P. Fang; C. H. Fan, A graphene nanoprobe for rapid, sensitive, and multicolor fluorescent DNA analysis. Adv Funct Mater. 2010;20:453-9.
[25] Y. Q. Wen; F. F. Xing; S. J. He; S. P. Song; L. H. Wang; Y. T. Long; D. Li; C. H. Fan, A graphene-based fluorescent nanoprobe for silver(I) ions detection by using graphene oxide and a silver-specific oligonucleotide. Chem Commun. 2010;46:2596-8.
[26] H. F. Dong; W. C. Gao; F. Yan; H. X. Ji; H. X. Ju, Fluorescence resonance energy transfer between quantum dots and graphene oxide for sensing biomolecules. Anal Chem. 2010;82:5511-7.
[27] F. Li; Y. Huang; Q. Yang; Z. T. Zhong; D. Li; L. H. Wang; S. P. Song; C. H. Fan, A graphene-enhanced molecular beacon for homogeneous DNA detection. Nanoscale. 2010;2:1021-6.
[28] F. Liu; J. Y. Choi; T. S. Seo, Graphene oxide arrays for detecting specific DNA hybridization by fluorescence resonance energy transfer. Biosens Bioelectron. 2010;25:2361-5.
[29] C. H. Lu; J. Li; J. J. Liu; H. H. Yang; X. Chen; G. N. Chen, Increasing the sensitivity and single-base mismatch selectivity of the molecular beacon using graphene oxide as the "nanoquencher". Chem Eur J. 2010;16:4889-94.
[30] H. X. Chang; L. H. Tang; Y. Wang; J. H. Jiang; J. H. Li, Graphene fluorescence resonance energy transfer aptasensor for the thrombin detection. Anal. Chem. 2010;82:2341-6.
[31] H. Jang; Y. K. Kim; H. M. Kwon; W. S. Yeo; D. E. Kim; D. H. Min, A graphene-based platform for the assay by helicase. Angew Chem Int Ed. 2010;49:5703-7.
[32] J. H. Jung; D. S. Cheon; F. Liu; K. B. Lee; T. S. Seo, A graphene oxide based immuno-biosensor for pathogen detection. Angew Chem Int Ed. 2010;49:5708-11.

[33] Y. J. Song; K. G. Qu; C. Zhao; J. S. Ren; X. G. Qu, Graphene oxide: Intrinsic peroxidase catalytic activity and its application to glucose detection. Adv Mater. 2010;22:2206-10.
[34] Y. Wang; Z. H. Li; D. H. Hu; C. T. Lin; J. H. Li; Y. H. Lin, Aptamer/graphene oxide nanocomplex for in situ molecular probing in living cells. J Am Chem Soc. 2010;132:9274-6.
[35] C.-H. Lu; J. Li; M.-H. Lin; Y.-W. Wang; H.-H. Yang; X. Chen; G.-N. Chen, Amplified aptamer-based assay through catalytic recycling of the analyte. Angew Chem Int Ed. 2010;49:8454-7.
[36] S. Xu; J. Zhan; B. Man; S. Jiang; W. Yue; S. Gao; C. Guo; H. Liu; Z. Li; J. Wang; Y. Zhou, Real-time reliable determination of binding kinetics of DNA hybridization using a multi-channel graphene biosensor. Nat Commun. 2017;8:14902.
[37] D. E. Huizenga; J. W. Szostak, A DNA aptamer that binds adenosine and ATP. Biochemistry. 1995;34:656-65.
[38] F. Zhang; J. Liu, Label-free colorimetric biosensors based on aptamers and gold nanoparticles: A critical review. Anal Sens. 2021;1:30-43.
[39] F. Zhang; P.-J. J. Huang; J. Liu, Sensing adenosine and atp by aptamers and gold nanoparticles: Opposite trends of color change from domination of target adsorption instead of aptamer binding. ACS Sensors. 2020;5:2885–93.
[40] C. Zong; J. Liu, The arsenic-binding aptamer cannot bind arsenic: Critical evaluation of aptamer selection and binding. Anal. Chem. 2019;91:10887-93.
[41] N. Varghese; U. Mogera; A. Govindaraj; A. Das; P. K. Maiti; A. K. Sood; C. N. R. Rao, Binding of DNA nucleobases and nucleosides with graphene. ChemPhysChem. 2009;10:206-10.
[42] J. Antony; S. Grimme, Structures and interaction energies of stacked graphene-nucleobase complexes. PCCP. 2008;10:2722-9.
[43] S. Gowtham; R. H. Scheicher; R. Ahuja; R. Pandey; S. P. Karna, Physisorption of nucleobases on graphene: Density-functional calculations. Phys Rev B. 2007;76:033401.
[44] C. Lu; P.-J. J. Huang; B. Liu; Y. Ying; J. Liu, Comparison of graphene oxide and reduced graphene oxide for DNA adsorption and sensing. Langmuir. 2016;32:10776–83.
[45] C. H. Lu; C. L. Zhu; J. Li; J. J. Liu; X. Chen; H. H. Yang, Using graphene to protect DNA from cleavage during cellular delivery. Chem Commun. 2010;46:3116-8.
[46] Z. W. Tang; H. Wu; J. R. Cort; G. W. Buchko; Y. Y. Zhang; Y. Y. Shao; I. A. Aksay; J. Liu; Y. H. Lin, Constraint of DNA on functionalized graphene improves its biostability and specificity. Small. 2010;6:1205-9.
[47] B. Liu; P.-J. J. Huang; E. Y. Kelly; J. Liu, Graphene oxide surface blocking agents can increase the DNA biosensor sensitivity. Biotechnol J. 2016;11:780-7.

Graphical abstract

